

LETTERS

The reversibility of mitotic exit in vertebrate cells

Tamara A. Potapova¹, John R. Daum¹, Bradley D. Pittman¹, Joanna R. Hudson¹, Tara N. Jones¹, David L. Satinover², P. Todd Stukenberg² & Gary J. Gorbsky¹

A guiding hypothesis for cell-cycle regulation asserts that regulated proteolysis constrains the directionality of certain cell-cycle transitions^{1,2}. Here we test this hypothesis for mitotic exit, which is regulated by degradation of the cyclin-dependent kinase 1 (Cdk1) activator, cyclin B³⁻⁵. Application of chemical Cdk1 inhibitors to cells in mitosis induces cytokinesis and other normal aspects of mitotic exit, including cyclin B degradation. However, chromatid segregation fails, resulting in entrapment of chromatin in the midbody. If cyclin B degradation is blocked with a proteasome inhibitor or by expression of non-degradable cyclin B, Cdk1 inhibitors will nonetheless induce mitotic exit and cytokinesis. However, if after mitotic exit, the Cdk1 inhibitor is washed free from cells in which cyclin B degradation is blocked, the cells can revert back to M phase. This reversal is characterized by chromosome recondensation, nuclear envelope breakdown, assembly of microtubules into a mitotic spindle, and in most cases, dissolution of the midbody, reopening of the cleavage furrow, and realignment of chromosomes at the metaphase plate. These findings demonstrate that proteasome-dependent degradation of cyclin B provides directionality for the M phase to G1 transition.

Cdk1, the major regulator of mitotic progression, is activated through binding of cyclin A or B. Cyclin A is degraded during prometaphase when chromosomes move to align at the metaphase plate^{6,7}. Cyclin B degradation begins at metaphase and continues during chromatid segregation in anaphase and exit from M phase⁵. Cytokinesis is initiated shortly after anaphase onset. Cdk1 inactivation and dephosphorylation of Cdk1 substrates during mitotic exit probably serve as timing mechanisms to ensure that cytokinesis occurs after chromatid separation⁸⁻¹². For example, high Cdk1 activity before anaphase blocks the accumulation of the cytokinetic regulators aurora B and MKLP1 at the cleavage furrow and on the microtubules of the spindle midzone¹³⁻¹⁵.

Flavopiridol is a potent inhibitor of Cdk1¹⁶. We found that treatment of vertebrate cells in mitosis with flavopiridol resulted in premature mitotic exit accompanied by cytokinesis (Fig. 1a and Supplementary Video 1). Similar results have recently been found for the Cdk inhibitor BMI-1026 (ref. 17). Flavopiridol induced the microtubule network to undergo changes characteristic of anaphase and mitotic exit. The spindle poles moved apart, and microtubule bundles formed in the spindle midzone and at the equatorial cortex. Even though chromatid separation did not occur, cytokinetic furrows formed and ingressed to completion. The cleavage furrow trapped chromosomes in the midbody, resulting in a 'cut' phenotype. Nevertheless, the chromosomes decondensed and nuclear envelopes reformed. Eventually, cytoplasmic contractile activity diminished as cells flattened fully onto the substratum, and the microtubule array established an interphase pattern.

During normal mitotic exit, Cdk1 activity is reduced by ubiquitylation and proteasome-mediated degradation of cyclin B^{3,5}. Proteasome inhibitors such as MG132 induce mitotic cells to arrest at

metaphase. We found that treatment with flavopiridol overrides metaphase arrest induced with MG132, causing mitotic exit and cytokinesis accompanied by chromosome decondensation and reformation of the nuclear envelope (Fig. 1b and Supplementary Video 2). The proteolysis of cyclin B at mitotic exit is thought to ensure the unidirectionality of the M phase to G1 transition². In cells with proteasome inhibition, we found that flavopiridol-induced mitotic exit was reversible. Upon flavopiridol removal, cells that had exited mitosis could return to metaphase (Fig. 1c and Supplementary Videos 3, 4). The microtubules, having assumed an interphase configuration after flavopiridol-induced mitotic exit, reassembled a mitotic spindle when flavopiridol was removed. The midbody disappeared and the cytokinetic furrow retracted, the newly formed nuclear envelope dissolved, and the chromosomes recondensed, attached to spindle microtubules and realigned at the metaphase plate. These findings are summarized in Supplementary Fig. 1. We found that cells induced to reverse back to metaphase could subsequently undergo a second, normal mitotic exit (including chromatid separation and movement) as well as a second cytokinesis if the proteasome inhibitor was subsequently washed away (Supplementary Video 5). We used flavopiridol for most of our experiments because of its high potency as a Cdk1 inhibitor (Supplementary Fig. 2). However, some other chemical Cdk1 inhibitors also resulted in similar phenotypes (see Supplementary Information).

In *Xenopus* S3 cells arrested at metaphase with MG132, aurora B kinase was concentrated at centromeres and MKLP1 was localized diffusely in the cytoplasm (Fig. 1d). Upon treatment with flavopiridol, aurora B and MKLP1 rapidly accumulated at the equatorial cell cortex, associating with the nascent cleavage furrows and the midzone overlaying the microtubule bundles, and eventually becoming highly concentrated at the midbody. These translocation events were consistent with the typical relocation of aurora B and MKLP1 in normal anaphase, and were also reversible: in cells that were induced through mitotic exit and then allowed to revert back to metaphase, aurora B and MKLP1 returned to their typical metaphase distributions (Fig. 1d, 60 min).

Metaphase cells treated with flavopiridol in the presence of proteasome inhibitor advanced through mitotic exit and cytokinesis, reaching the midbody stage with decondensed chromosomes and reassembled nuclear envelopes 25 min after treatment (Fig. 1b). The reversibility of mitotic exit was dependent on the duration of exposure to flavopiridol. Treatment with 5 μ M for 17–30 min resulted in most cells (81 out of 106) returning to metaphase upon flavopiridol washout (Table 1). With longer exposure to flavopiridol, the proportion of cells that underwent reversal declined. However, a few cells (3 out of 24) still reversed when flavopiridol was removed 80 min after its addition. We detected no reversal among cells treated for 90 min ($n = 26$). Reversibility was entirely dependent on the presence of the proteasome inhibitor. In medium without

¹Program in Molecular, Cell and Developmental Biology, Oklahoma Medical Research Foundation, 825 NE 13th Street, Oklahoma City, Oklahoma 73104, USA. ²Department of Biochemistry and Molecular Genetics, University of Virginia Medical School, 1300 Jefferson Park Avenue, Charlottesville, Virginia 22908, USA.

proteasome inhibitor, premature mitotic exit and cytokinesis induced with flavopiridol did not reverse in any of 13 prometaphase cells when the flavopiridol was removed at 17–20 min.

Previous studies have shown that several early mitotic regulators (for example, cyclin A) are normally degraded during prophase and prometaphase, as well as during the prometaphase arrest induced with microtubule drugs^{6,7}. We treated *Xenopus* S3 cells with the microtubule drug nocodazole to allow degradation of early mitotic regulators. Cells were then released from nocodazole to medium containing proteasome inhibitor. The cells assembled spindles and arrested at metaphase, but were fully capable of undergoing flavopiridol-induced mitotic exit and reversal (Fig. 2a and Supplementary Video 6). This result is consistent with the interpretation that mitotic exit reversal in cells treated with proteasome inhibitor is due to the protection of cyclin B from degradation, not due to the preservation of early mitotic regulators.

We next measured cell-cycle markers during induced mitotic exit and reversal. We treated nocodazole-arrested HeLa cells with flavopiridol according to the scheme depicted in Fig. 2b. We then calculated mitotic indices from the percentage of cells with condensed chromosomes (Fig. 2c, top), and immunoblotted samples for

various cell-cycle markers (Fig. 2c, bottom). Although the level of Cdk1 protein remained constant, flavopiridol induced mitotic exit and degradation of cyclins B1 and B2 in the absence of the proteasome inhibitor MG132 (Group 3, –MG132). In medium containing MG132, flavopiridol induced mitotic exit, but cyclin B1 and B2 were preserved (Group 3, +MG132). Flavopiridol removal at 25 min caused reversal back to M phase in the presence of MG132 (Group 5, +MG132, asterisk) but not in its absence (Group 5, –MG132). As expected, cyclin A, prominent when the initial population of mitotic cells was analysed (Group 1, –45 min), was substantially degraded during the subsequent 45 min incubation period before flavopiridol addition (Group 2). When flavopiridol was removed at 25 min in the mitotic exit reversal experiments, cyclin A levels were very low (Group 3) and thus unlikely to contribute significantly to the reactivation of Cdk1. After longer treatments with flavopiridol, some re-synthesis of cyclin A protein seemed to occur in cells treated with MG132 (Groups 4 and 5, +MG132). In summary, reversal of mitotic exit after flavopiridol removal correlates with the preservation of cyclins B1 and B2.

Flavopiridol was an effective inhibitor when purified Cdk1/cyclinB complex was used to phosphorylate histone H1 *in vitro*, showing

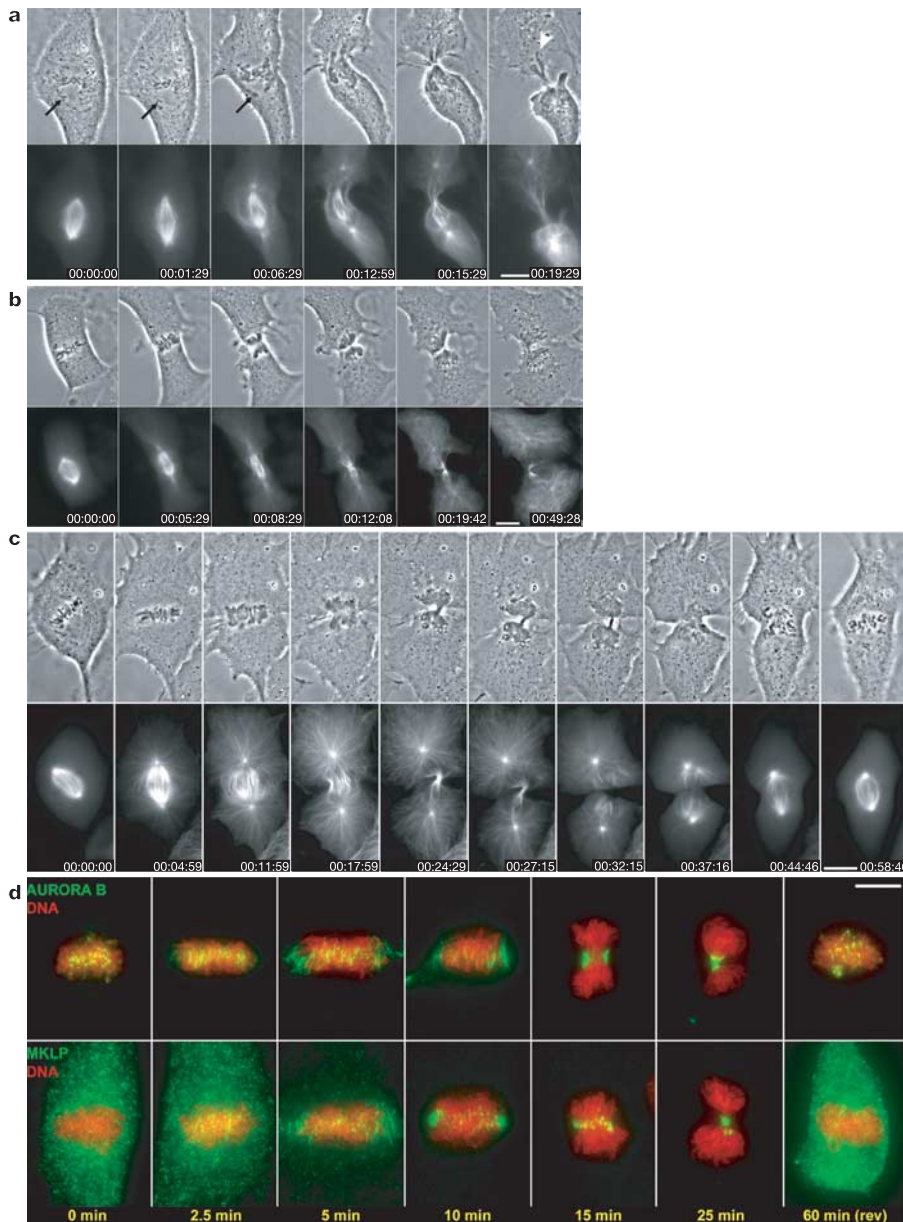


Figure 1 | The Cdk inhibitor flavopiridol induces reversible mitotic exit and cytokinesis if proteasome activity is inhibited. **a**, Treatment of mitotic cells with flavopiridol induces premature mitotic exit and cytokinesis without chromatid separation. A *Xenopus* S3 cell expressing α -tubulin–GFP was treated with 5 μ M flavopiridol at time 0. The black arrow indicates a chromosome not yet at metaphase when flavopiridol was added. The white arrowhead indicates the reassembled nuclear envelope. Supplementary Video 1 shows the complete video sequence. **b**, Flavopiridol induces mitotic exit in cells arrested at metaphase with MG132. An MG132-arrested cell was treated with 10 μ M flavopiridol at time 0. Supplementary Video 2 shows the complete video sequence. **c**, Flavopiridol-induced mitotic exit and cytokinesis are reversible if the proteasome is inhibited. An MG132-arrested cell was treated with 5 μ M flavopiridol at time 0, and flavopiridol was removed at 25 min. Supplementary Video 3 shows the complete video sequence. The top panels in **a–c** show phase-contrast images, and the bottom panels show α -tubulin–GFP fluorescence. Time in **a–c** is indicated as hours:minutes:seconds. **d**, Flavopiridol induces normal mitotic exit changes in the distributions of aurora B kinase and MKLP1. These are reversible upon flavopiridol removal. *Xenopus* S3 cells were incubated in medium containing MG132 and were fixed before and after treatment with 5 μ M flavopiridol. Samples were labelled for aurora B kinase (top panels) or MKLP1 (bottom panels). First and last images (0 min and 60 min) were scaled identically for brightness and contrast. Other images were scaled individually. Scale bars, 10 μ m.

Table 1 | Reversal of mitotic exit in *Xenopus* S3 cells upon removal of flavopiridol

Duration of flavopiridol treatment (min)	Number of cells imaged	Number of cells reversed through mitotic exit (% reversed)
17	29	28 (97)
20	27	25 (93)
25	27	17 (63)
30	23	11 (48)
33–37	17	8 (47)
40	22	6 (27)
50	19	4 (21)
60	17	1 (6)
70	24	1 (4)
80	24	3 (12)
90	26	0 (0)

higher potency than certain commonly used Cdk1 inhibitors such as olomoucine and roscovitine (Supplementary Fig. 2). In living cells, flavopiridol resulted in dephosphorylation of known Cdk1 substrates. In both the presence and absence of MG132, flavopiridol eliminated labelling with the TG-3 antibody that recognizes a Cdk1-catalysed phospho-epitope on nucleolin¹⁸ (Group 3). Cdh1, an activator of the mitotic ubiquitin ligase APC/C, is inhibited by Cdk1 phosphorylation during M phase¹⁹. Flavopiridol treatment resulted in an increase in the electrophoretic mobility of Cdh1, but only in the absence of MG132. Cdh1 dephosphorylation may be involved in the ubiquitylation and breakdown of cyclin B after flavopiridol treatment in the absence of MG132 (Group 3, -MG132).

Like *Xenopus* S3 cells, HeLa cells cultured in MG132 underwent a defined period after flavopiridol-induced mitotic exit when removal of flavopiridol led to reversal back to metaphase. When flavopiridol was removed 25 min after its addition, all cells (10 out of 10) reversed back to metaphase. When removed at 60 min, only 2 out of 12 cells (17%) underwent reversal.

To test whether preservation of cyclin B alone was sufficient for reversal of mitotic exit and cytokinesis, we performed a series of experiments using non-degradable cyclin B1 fused to green fluorescent protein (cyclinB1(R42A)-GFP) in place of the proteasome inhibitor. Most HeLa cells expressing non-degradable cyclin B arrested at metaphase, as has previously been shown¹². When these metaphase-arrested cells were treated with flavopiridol, they completed cytokinesis and exited mitosis. In some cells, flavopiridol treatment also induced chromatids to separate and to move to the poles before mitotic exit and cytokinesis. When flavopiridol was removed 25 min after its addition, 17 out of 37 transfected cells reverted back to M phase. In all 17 cells that underwent mitotic exit reversal, the chromosomes recondensed within 10 min of flavopiridol removal. Cells that had not separated their chromatids opened their cleavage furrows rapidly (average time, 13 min after flavopiridol removal) and reversed back to metaphase within 30 min (Fig. 3a and Supplementary Video 7). Flavopiridol addition induced chromatid separation in 7 of the 17 cells that subsequently underwent mitotic exit reversal. In these cells, the chromatids recondensed rapidly (within 10 min of flavopiridol removal) but opening of the cleavage furrow was somewhat delayed (average time 45 min after flavopiridol removal) (Fig. 3b and Supplementary Video 8). The separated chromatids remained near the centre of the cell but did not realign to form a metaphase plate. Two of the seven cells with separated chromatids did not show evidence of reopening their cleavage furrows at our final observation time (90 min after flavopiridol removal). Thus, cells with separated chromatids can undergo reversal of mitotic exit and cytokinesis, but predictably, the chromatids cannot realign at the metaphase plate if the sister chromatids have lost cohesion. Moreover, although cytokinesis is still reversible after chromatid segregation, reopening of the cleavage furrow generally takes longer to initiate. Trapped chromatin might physically facilitate re-opening of the furrow, or cells that separate their chromatids may have biochemical differences that restrict furrow

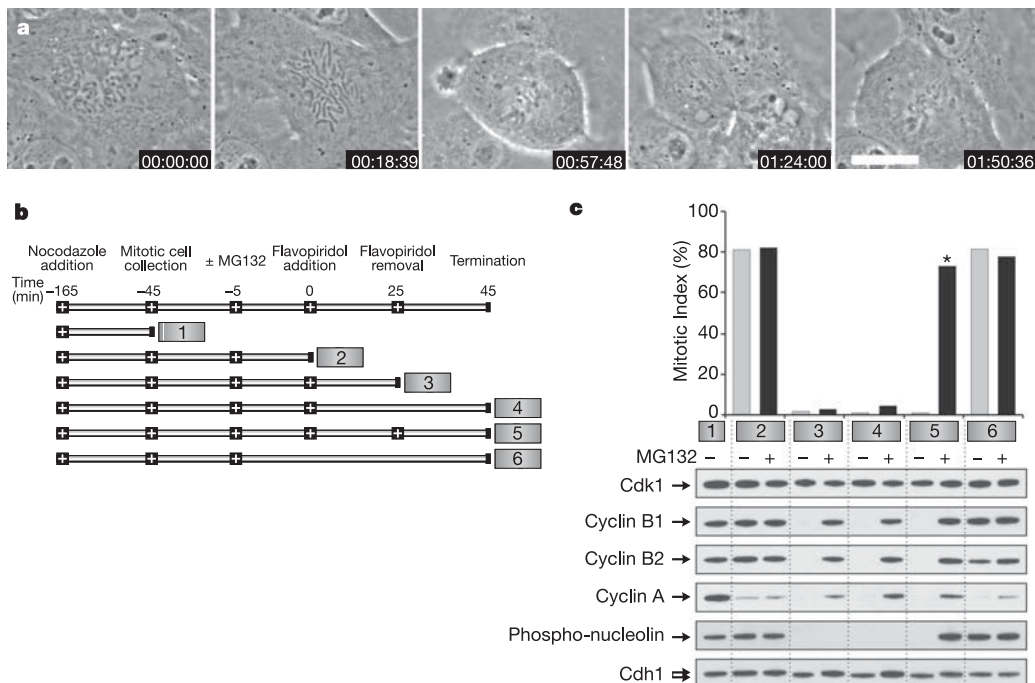


Figure 2 | Reversibility of mitotic exit requires preservation of cyclin B. **a**, A *Xenopus* S3 cell treated with 100 ng ml⁻¹ nocodazole at time 0. Nocodazole was removed 30 min after nuclear envelope breakdown, and the cell was arrested at metaphase with the addition of MG132. Flavopiridol at 5 μM was added at 1:04:00 and removed 25 min later, after mitotic exit. Supplementary Video 6 shows the complete video sequence. Scale bar,

10 μm. **b**, Experimental protocol used for producing samples from HeLa cells at various stages of induction and reversal of mitotic exit. **c**, Samples were analysed for mitotic index (the proportion of cells undergoing mitosis) and blotted for the indicated proteins. Asterisk indicates population that underwent mitotic exit reversal.

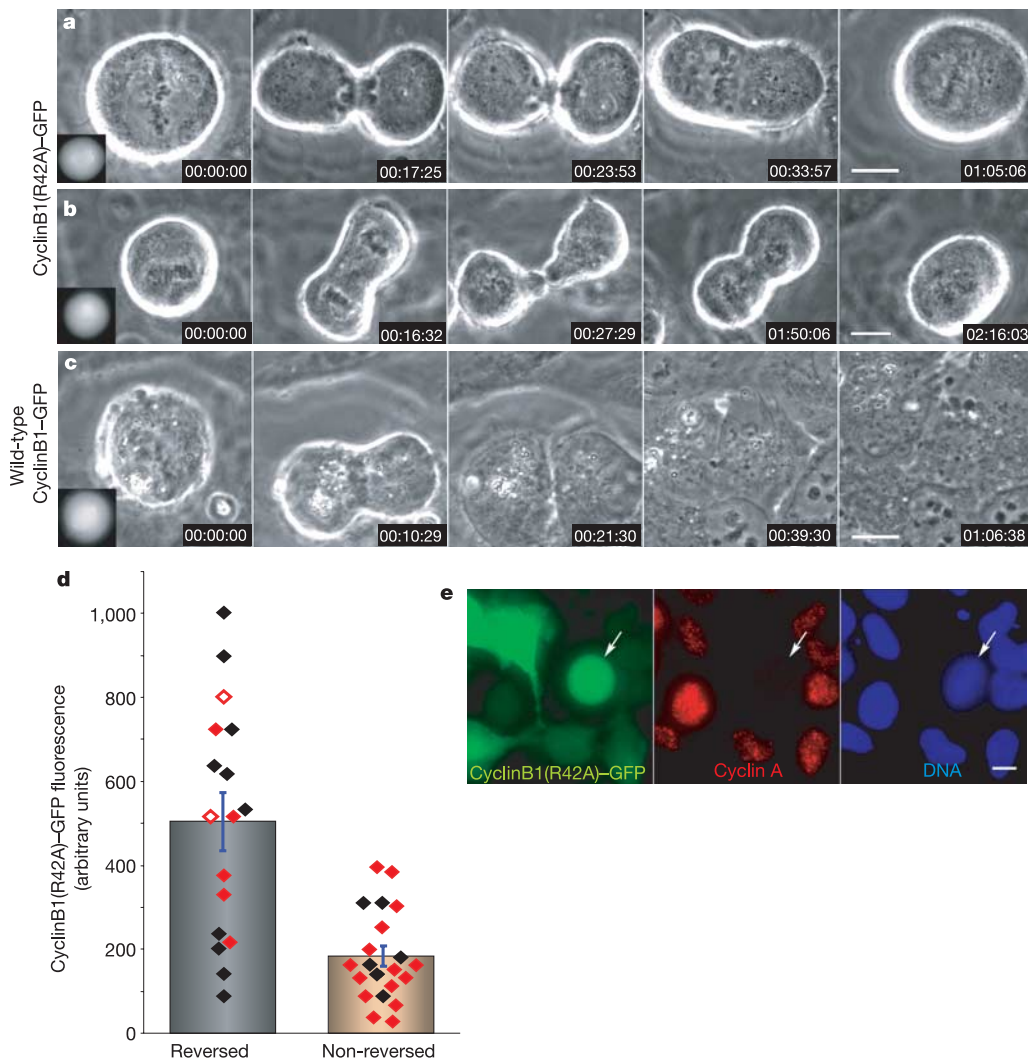


Figure 3 | Cells expressing non-degradable cyclin B1 undergo mitotic exit reversal. **a**, HeLa cells expressing non-degradable cyclin B1 can undergo mitotic exit reversal without segregating chromosomes. Flavopiridol was added at time 0 and removed at 25 min. Supplementary Video 7 shows the complete video sequence. **b**, HeLa cells expressing non-degradable cyclin B1 can undergo mitotic exit reversal after chromatid separation. Flavopiridol added and removed as in **a**. Supplementary Video 8 shows the complete video sequence. **c**, HeLa cells expressing wild-type cyclin B1 do not undergo reversal of mitotic exit. Flavopiridol added and removed as in **a**. Supplementary Video 9 shows the complete video sequence. Insets show GFP fluorescence images at

time 0. The level of wild-type cyclin B1 in **c** is approximately twice that of the non-degradable cyclin B1 expressed in **a** and **b**. **d**, Cells expressing high levels of non-degradable cyclin B1 are more likely to undergo mitotic exit reversal. Black diamonds indicate cells that did not separate chromatids upon treatment with flavopiridol, red diamonds show cells with separated chromatids. Open red diamonds indicate two cells that recondensed their chromosomes but had not opened their cleavage furrows by 90 min after flavopiridol removal. Error bars show s.e.m. **e**, A mitotic HeLa cell at metaphase (arrow) expressing non-degradable cyclin B1 has low levels of cyclin A expression, as assessed by immunofluorescence. Scale bars, 10 μ m.

re-opening. Mitotic cells expressing high levels of wild-type cyclin B fused to GFP underwent mitotic exit and cytokinesis upon flavopiridol treatment, but as expected, removing flavopiridol after 25 min never resulted in reversal of mitotic exit ($n = 6$) (Fig. 3c and Supplementary Video 9).

Cells expressing high levels of non-degradable cyclin B (as measured by GFP fluorescence) were more likely to undergo reversal than those expressing low levels (Fig. 3d). Previous work suggests that cell-cycle regulation in M phase shows the property of hysteresis, because entry into M phase from G2 requires higher Cdk1 activity

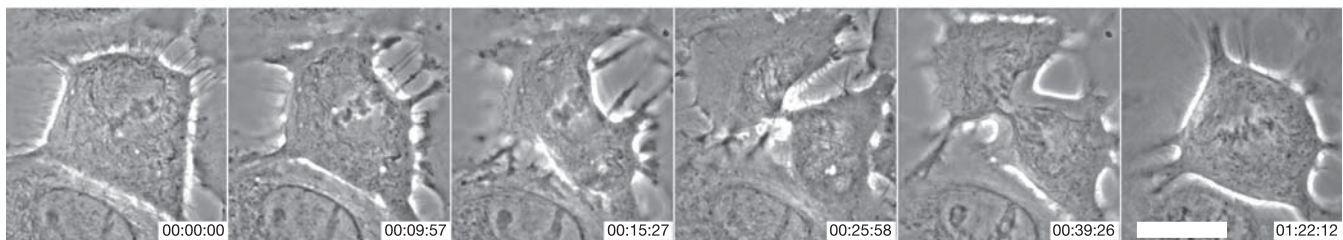


Figure 4 | Primary cultures of human cells can undergo mitotic exit reversal. An MG132-arrested metaphase human keratinocyte was imaged by phase-contrast microscopy after addition of 7.5 μ M flavopiridol at time 0.

The flavopiridol was removed at 26 min. Supplementary Video 10 shows the complete video sequence. Scale bar, 10 μ m.

than does maintaining M phase once it is achieved^{20,21}. This hysteresis might explain why many cells expressing relatively low levels of non-degradable cyclin B arrested at metaphase before flavopiridol treatment, but were unable to undergo reversal when flavopiridol was removed. Additionally, in confirmation of our previous conclusion that the reversal of mitotic exit and the re-establishment of high Cdk1 activity levels in the presence of proteasome inhibitor are probably driven by cyclin B and not cyclin A, we found that cells arrested at metaphase by expression of non-degradable cyclin B had nearly undetectable levels of cyclin A (Fig. 3e).

The above studies were all completed using immortalized cell lines. To determine whether these findings are broadly applicable to non-immortalized cells, we also tested primary human keratinocytes. We found that these cells, cultured in medium containing MG132, undergo mitotic exit and cytokinesis in response to flavopiridol treatment, and reverse back to metaphase when flavopiridol is removed (Fig. 4 and Supplementary Video 10).

The importance of regulated proteolysis for guiding the directionality of cell-cycle transitions is a central tenet of modern cell-cycle theory, extended from founding work on proteolysis of cyclins in early embryos^{1–4,22}. Here we have tested this idea and shown that if cyclin B is stabilized, the events of mitotic exit and cytokinesis are immediately reversible, even in cells that have progressed through chromosome decondensation, reconstitution of the interphase nucleus, mitotic spindle disassembly and cytokinesis to the stage of midbody formation. However, with increasing time after flavopiridol-induced mitotic exit, this reversibility wanes. Thus, cyclin degradation does provide directionality during mitotic exit, but this function must later be supplemented by other events that inhibit backtracking. These events are likely to involve other biochemical changes to Cdk1, including phosphorylation changes or the binding of small-molecule inhibitors. The ability to regulate mitotic exit in the absence of cyclin degradation in vertebrate cells will facilitate elucidation of the downstream regulators of the M to G1 phase transition in vertebrate cells.

METHODS

Cell culture and live cell imaging. *Xenopus* S3 cells stably expressing α -tubulin-GFP were grown at 23°C in 70% L-15 medium supplemented with 15% fetal bovine serum. See Supplementary Video 12 for control images of these cells transiting M phase. HeLa cells were grown in DMEM medium with 10% FBS in 5% CO₂ at 37°C. Normal human epidermal keratinocytes (Clonectics) were grown in defined keratinocyte SFM medium (Invitrogen). Time-lapse phase-contrast and fluorescence images were collected from cells grown on glass coverslips using a Zeiss Axiovert 200M microscope equipped with a Hamamatsu ORCA camera. When applicable, cells were incubated for 30–60 min with 25 μ M MG132 (Calbiochem) or with 100 ng ml⁻¹ nocodazole (Sigma). Flavopiridol was provided by the National Cancer Institute (Drug Synthesis and Chemistry Branch, Developmental Therapeutics Program, Division of Cancer Treatment and Diagnosis) and used at 5–10 μ M. In cells expressing cyclin B1-GFP, expression levels were quantified using Metamorph software (Molecular Devices).

Immunofluorescence and immunoblotting. Cells on coverslips were fixed in 2–3% formaldehyde in PHEM buffer (60 mM PIPES, 25 mM HEPES (pH 6.8), 10 mM EDTA, 4 mM MgCl₂) for 15 min, then permeabilized with 0.5% or 1% Triton X-100. HeLa cells in suspension were fixed in PHEM buffer containing 1.5% formaldehyde and 0.5% Triton X-100. Antibodies against *Xenopus* MKLP1 and aurora B were prepared in rabbits. Mouse antibody against human cyclin A was obtained from J. Gannon and T. Hunt, or obtained commercially (Abcam). Fluorescence images were taken using a Zeiss Axioplan II microscope with a Hamamatsu ORCA-II camera. Samples were treated with 4,6-diamidino-2-phenylindole (DAPI) and mounted in Vectashield containing 10 mM MgSO₄.

For immunoblotting, cells were lysed in NuPAGE western blotting sample buffer (Invitrogen) containing 50 mM dithiothreitol. Samples were electrophoresed on 4–12% gradient gels, transferred to PVDF membranes and probed with primary antibodies overnight at 4°C. Blots were then treated with

appropriate HRP-conjugated secondary antibodies, and developed using SuperSignal West Pico chemiluminescent substrate (Pierce).

Received 30 December 2005; accepted 13 February 2006.

1. Minshull, J. *et al.* The role of cyclin synthesis, modification and destruction in the control of cell division. *J. Cell Sci.* 12 (suppl.), 77–97 (1989).
2. Reed, S. I. Ratchets and clocks: the cell cycle, ubiquitylation and protein turnover. *Nature Rev. Mol. Cell Biol.* 4, 855–864 (2003).
3. Glotzer, M., Murray, A. W. & Kirschner, M. W. Cyclin is degraded by the ubiquitin pathway. *Nature* 349, 132–138 (1991).
4. Murray, A. W. & Kirschner, M. W. Cyclin synthesis drives the early embryonic cell cycle. *Nature* 339, 275–280 (1989).
5. Clute, P. & Pines, J. Temporal and spatial control of cyclin B1 destruction in metaphase. *Nature Cell Biol.* 1, 82–87 (1999).
6. Geley, S. *et al.* Anaphase-promoting complex/cyclosome-dependent proteolysis of human cyclin A starts at the beginning of mitosis and is not subject to the spindle assembly checkpoint. *J. Cell Biol.* 153, 137–148 (2001).
7. den Elzen, N. & Pines, J. Cyclin A is destroyed in prometaphase and can delay chromosome alignment and anaphase. *J. Cell Biol.* 153, 121–136 (2001).
8. Cross, F. R., Schroeder, L., Kruse, M. & Chen, K. C. Quantitative characterization of a mitotic cyclin threshold regulating exit from mitosis. *Mol. Biol. Cell* 16, 2129–2138 (2005).
9. Parry, D. H. & O'Farrell, P. H. The schedule of destruction of three mitotic cyclins can dictate the timing of events during exit from mitosis. *Curr. Biol.* 11, 671–683 (2001).
10. Sigrist, S., Jacobs, H., Stratmann, R. & Lehner, C. F. Exit from mitosis is regulated by *Drosophila* fizzy and the sequential destruction of cyclins A, B and B3. *EMBO J.* 14, 4827–4838 (1995).
11. Visintin, R. *et al.* The phosphatase Cdc14 triggers mitotic exit by reversal of Cdk-dependent phosphorylation. *Mol. Cell* 2, 709–718 (1998).
12. Chang, D. C., Xu, N. & Luo, K. Q. Degradation of cyclin B is required for the onset of anaphase in mammalian cells. *J. Biol. Chem.* 278, 37865–37873 (2003).
13. Carmena, M. & Earnshaw, W. C. The cellular geography of aurora kinases. *Nature Rev. Mol. Cell Biol.* 4, 842–854 (2003).
14. Glotzer, M. The molecular requirements for cytokinesis. *Science* 307, 1735–1739 (2005).
15. Mishima, M., Pavicic, V., Gruneberg, U., Nigg, E. A. & Glotzer, M. Cell cycle regulation of central spindle assembly. *Nature* 430, 908–913 (2004).
16. Losiewicz, M. D., Carlson, B. A., Kaur, G., Sausville, E. A. & Worland, P. J. Potent inhibition of CDC2 kinase activity by the flavonoid L86–8275. *Biochem. Biophys. Res. Commun.* 201, 589–595 (1994).
17. Niiya, F., Xie, X., Lee, K. S., Inoue, H. & Miki, T. Inhibition of cyclin-dependent kinase 1 induces cytokinesis without chromosome segregation in an ECT2 and MgcRacGAP-dependent manner. *J. Biol. Chem.* 280, 36502–36509 (2005).
18. Dranovsky, A. *et al.* Cdc2 phosphorylation of nucleolin demarcates mitotic stages and Alzheimer's disease pathology. *Neurobiol. Aging* 22, 517–528 (2001).
19. Kramer, E. R., Scheuringer, N., Podtelejnikov, A. V., Mann, M. & Peters, J. M. Mitotic regulation of the APC activator proteins CDC20 and CDH1. *Mol. Biol. Cell* 11, 1555–1569 (2000).
20. Pomeroy, J. R., Sontag, E. D. & Ferrell, J. E. Jr. Building a cell cycle oscillator: hysteresis and bistability in the activation of Cdc2. *Nature Cell Biol.* 5, 346–351 (2003).
21. Sha, W. *et al.* Hysteresis drives cell-cycle transitions in *Xenopus laevis* egg extracts. *Proc. Natl Acad. Sci. USA* 100, 975–980 (2003).
22. Evans, T., Rosenthal, E. T., Youngblom, J., Distel, D. & Hunt, T. Cyclin: a protein specified by maternal mRNA in sea urchin eggs that is destroyed at each cleavage division. *Cell* 33, 389–396 (1983).

Supplementary Information is linked to the online version of the paper at www.nature.com/nature. A summary figure is also included.

Acknowledgements We thank the staff at the OMRF Imaging Center and W. Martin for technical assistance. We thank Sanofi-Aventis Pharmaceuticals and the National Cancer Institute for providing flavopiridol. We thank J. Pines for providing cyclin B plasmids and P. Davies for TG-3 anti-phospho-nucleolin antibody. We thank J. Gannon and T. Hunt for antibodies against Cdk1 and cyclins. This work was supported by grants from the National Institutes of Health (to G.J.G. and P.T.S.), from the American Cancer Society (to P.T.S.) and from an NIH training grant (to D.L.S.).

Author Information Reprints and permissions information is available at npg.nature.com/reprintsandpermissions. The authors declare no competing financial interests. Correspondence and requests for materials should be addressed to G.J.G. (GJG@omrf.ouhsc.edu).